Photocatalytic activity of titania films produced with plasma electrolytic oxidation

A. E. R. Friedemann[a b c*], K. Thiel[a], Th. M. Gesing[b c], P. Plagemann[a]

[a]FRAUNHOFER Institute for Manufacturimg Technology and Advanced Materials IFAM, Wiener Straße 12, D-28359 Bremen, Germany

[b]University of Bremen, Institute of Inorganic Chemistry and Crystallography, Leobener Straße 7, D-28359 Bremen, Germany

[c]University of Bremen, MAPEX Center for Materials and Processes, Bibliothekstraße 1, D-28359 Bremen, Germany

* Corresponding author. Tel.: +49 421 2246-7365;
E-mail address: ariane.friedemann@ifam.fraunhofer.de (A. E. R. Friedemann).

Abstract

The photocatalytic activity of titanium dioxide (TiO_2) results from its crystalline phase's anatase and rutile. In this regard, plasma electrolytic oxidation (PEO) is a promising process for producing highly porous surfaces with a high proportion of crystalline phases into the oxide layer on pure titanium. PEO-coatings were produced under different conditions in various electrolytes in order to identify the crystalline fractions of the surfaces and to examine the associated photocatalytic activity. The composition of the PEO electrolyte was varied to optimize the polymorphic composition of the TiO_2 comparable to the photocatalytic active TiO_2 material AEROXIDE® P25. X-ray powder diffraction (XRD) was selected to identify the produced crystal structures of anatase and rutile on the surface material depending on the electrolytic system. In order to establish the expected band gap of the titanium dioxides on the surfaces, the samples were subjected to a diffuse reflectance measurement, which detected direct transitions for all samples using the TAUC and DASF methods. The acceptance of the photocatalytic reaction by the crystalline PEO-samples was further confirmed by the degradation of two typical dyes (methylene blue MB, rhodamine B RB) under UV-light irradiation. Both a high proportion of anatase and the presence of rutile on the PEO-layers had a targeted effect on the catalytic efficiency. However, the average crystallite sizes also played an important role in the samples produced in an optimum range of 30 - 40 nm. Both effects support the photocatalytic properties of PEO-surfaces.

Keywords: Plasma electrolytic oxidation, TiO_2 layer, Anatase, Rutile, Crystallinity, Photocatalytic activity

1 Introduction

With the current high levels of energy consumption and the necessity of developing ecological disposal methods, photo-catalysis has been the focus of scientific research as a gentle method for removing organic or inorganic pollutants [1–3] and for the generation of renewable energies [4–7]. Due to the high efficiency in this area, semiconducting compounds have been shown to be very useful. Of these, TiO_2 is considered to be one of the most successful photo-catalysts due to its high oxidizing ability and the rapid generation of excitons (electron hole pairs), because of its high photon-absorbing property with band gap energies of E_g = 3.2 eV for anatase and E_g = 3.0 eV for rutile. Many parameters act on the photocatalytic activity of TiO_2 such as the phase composition, average crystallite size, particle size, surface area, crystallinity of the phases, impurities and absorption or desorption of molecules [8–11]. Anatase is apparently the most photocatalytic active polymorph of TiO_2 and has played an important role in many ongoing investigations on titania products over the last few years. On the other hand, studies on the influence of rutile during photocatalytic reactions are not extensive [12–17].

Normally, photocatalytic experiments are carried out with nano-particulate powder samples, which are significantly crystalline as their high surface area enables a high absorption of photons on the surface [18,19]. There are many different methods of forming titania layers, such as sol-gel [20], dip-coating [21], thermal sintering or chemical vapor deposition [22,23]. To combine crystallinity and a huge surface area, plasma electrolytic oxidation (PEO) (also called: micro arc oxidation (MAO), plasma chemical oxidation, micro plasma oxidation or spark anodizing) is a suitable process of forming titania layers with a high porosity showing both anatase and rutile phases. This type of process has been used industrially since the 1960s [24–27]. Several local micro discharges with a high temperature increase and energy input over the entire metal surface result in the formation of partially crystalline TiO_2 polymorphs, which also allows a high layer thickness and surface due to the emerging pore density [28]. During the last few years the context of photo-catalysis and PEO has been reported [29–33]. The effect of crystallinity and TiO_2 phase composition on PEO-surfaces has not yet been fully investigated. Light quanta are generated by the illumination of the titanium oxides anatase and rutile with UV-light, causing excitation of the electrons in the conduction band. During the excitation the electron generates a hole in the valence band and this hole can be filled by some electron donors at the surface of the particles. Also, the oxidative holes can capture an electron from the existing organic compounds [8,34]. However, the optimization of photocatalytic activity with PEO-generated surfaces has not yet been fully investigated.

In comparison to our previous investigation [35], this study was carried out to optimize the crystalline parts of the titania layer with the PEO-process using different electrolytic systems and voltages. These two parameters were used to create, on one hand, an anatase-rich surface and, on the other hand, an anatase and rutile-containing surface with a ratio nearly identical to the commercially available AEROXIDE® P25. AEROXIDE® P25 shows very high photocatalytic behavior and is used

as a reference. The degradation reactions were carried out with two typical organic dyes (Methylene blue, Rhodamine B) to compare and exclude any interfering reactions at the TiO_2 surfaces. Prior to the photocatalytic investigation, all produced samples were examined for their TiO_2 band gap. Due to the variety of parameters act on the photocatalytic activity in this study it was focused on the crystallinity and composition of TiO_2 polymorphs in the PEO-surfaces.

2 Experimental procedures

2.1 Preparation of titania films

The rectangular titanium samples (cp Ti, grade 1) with the dimensions 150 x 100 mm^2 were cleaned with a solution of SurTec®152 and etched with Turco®5578 prior to oxidation to remove the natural oxide layer. The samples were rinsed with pure water and afterwards oxidized in the chosen electrolytes. Different aqueous electrolytes, as listed in Tab. 1, were used to produce the PEO titania layers. The electrolytes were maintained at a temperature of 295 ± 10 K by re-circulation through a chemical pump and an ice cooled beaker and stirred with a digital magnetic stirrer (IKA-Werke GmbH & Co. KG, Staufen, Germany). The experiments were performed with a two electrode circuit and a commercially available power supply EA PS 8360 15T (0 – 360 V, 0 – 15 A, 1500 W, EA Elektro-Automatik GmbH & Co. KG Viersen, Germany). The voltage ramp and holding time (total 18 min) was set using the software UTA 12 (Fraunhofer IFAM Bremen, Germany). Finally, the PEO-samples were rinsed in demineralized water and air-dried.

Tab. 1: Contents of the used electrolytes

Electrolyte	Concentration	PEO Voltages /V
E 1	0.3 M H_3PO_4, 1.5 M H_2SO_4	220, 280
E 2	0.2 M $Ca(C_2H_3O_2)_2$, 0.02 M $NaC_3H_7O_6P$	300
E 3	1.5 M H_2SO_4	130, 140
E 5	0.5 M NaOH, 0.2 M $C_4H_4Na_2O_6$	105, 115

2.2 Investigation of crystallinity and structural analysis

The crystallinity of the titania layers was examined by X-ray diffraction (XRD) analysis on a Xpert MPD powder diffractometer (PANalytical, Kassel, Germany) with Ni-filtered Cu-$K\alpha_{1,2}$-radiation ($\lambda_{K\alpha1}$ = 154.05929(5) pm, $\lambda_{K\alpha2}$ = 154.4414(2) pm) in Bragg-Brentano geometry. The samples were measured from 20° to 100° 2θ with a step-size of 0.0167° per 3 s. Scanning electron microscopy (SEM) was used to clarify the surface structure, carried out in a FEI Helios 600 Dual-Beam (Oregon, USA) field emission scanning electron microscope (FESEM) (Thermo Fisher Scientific, Hillsboro, USA) in the BSE mode. To investigate the oxide layer thickness the focused ion beam (FIB) analysis was used. Before measuring the samples were covered with a 1 µm platinum layer by means of ion beam induced deposition to protect the surfaces from the following ion bombardment. The protection layer can be seen on top of the oxide layer in all cross-section micrographs. Usually when preparing cross-sections in the FIB samples are tilted 52° that the ion beam is parallel to the surface normal. Hence, the electron beam is not perpendicular to the surface of the cross-section under this geometry. The resulting foreshortening of the y-axis was corrected in the microscope software for all

measurements of oxide thicknesses. Depending on the chosen mode an Everhart-Thornley or a ThruLense-Detector was used for imaging.

2.3 Band gap measurement

The band gaps of the produced PEO-samples were determined from UV-Vis diffuse reflectance spectra. The spectra were recorded on a Shimadzu UV-Vis spectrophotometer UV-2600 (Duisburg, Germany) equipped with an ISR-2600 plus a two-detector integrating sphere. Barium sulfate was used as a reference and was measured before the series to smooth the background. The data were collected from 200 to 1400 nm in 0.5 nm steps.

2.4 Photo degradation reactions

The PEO-samples were investigated regarding their photocatalytic activity by observing the degradation of the aqueous solution of two typical dyes under UV-light. Methylene blue (MB, AppliChem GmbH, Darmstadt, Germany) and rhodamine B (RB, AppliChem GmbH, Darmstadt, Germany) were used. To determine the change in absorption of the two dyes, a UV/Vis-spectrometer Cary®50 Conc (Varian Inc., Agilent Technologies, Santa Clara, USA) was used. Changes in absorption intensity were based on the Lambert-Beer equation (I: Intensity of transmitted light, I_0: Intensity of irradiated light, c: concentration, ε: extinction coefficient, d: layer thickness).

$$E = lg\left(\frac{I_0}{I}\right) = \varepsilon \cdot c \cdot d \quad (1)$$

The region from 450 nm to 800 nm was chosen because methylene blue has an absorption peak at 664 nm [32,34]. For rhodamine B, the region of 400 nm to 700 nm was chosen because of an absorption peak at 554 nm [36]. The PEO-samples were immersed in 3 mL of a prepared 37 mM MB solution and a 0.005 mM RB solution and irradiated with a 25 W UV-lamp (black light, Phillips, Germany). After 1 day, a solution of each sample was measured with the UV/Vis-spectrometer. To exclude some adsorption or desorption effects one untreated titanium plate was measured. Also, one PEO-treated sample was left in the dark and the dye solutions were irradiated without a sample. P25 is used as a reference because of its proven optimal photocatalytic behavior and it allows a comparison of the strength in photocatalytic behavior for the PEO-surfaces.

3 Results and discussion

3.1 Film characterization and crystallinity

The SEM images of the photocatalytic active titania films prepared with the PEO-process (section 2.2) are shown in Fig. 1. The topographies of the different layers display a characteristic rough and pore-rich structure comparable to [32,37–40]. The acidic electrolytes E1 and the alkaline electrolyte E2 generated a high pore density with a pore diameter of 1.5 - 3.0 µm, which has only been reported for phosphate-containing electrolytes [30,31,37,39–41]. In contrast, the electrolyte E3 and E5 produce a more stacked oxide layer containing holes instead of pores, showing a “pore” diameter of 1.0 - 1.3 µm. The determined pore sizes of the different surfaces are summarized in Tab. 2. To analyze the phase composition of the layers, the diffraction patterns of the PEO-surfaces were measured (Fig. 2). The analyzed crystalline phases on the PEO-surfaces are also given in Tab. 2.

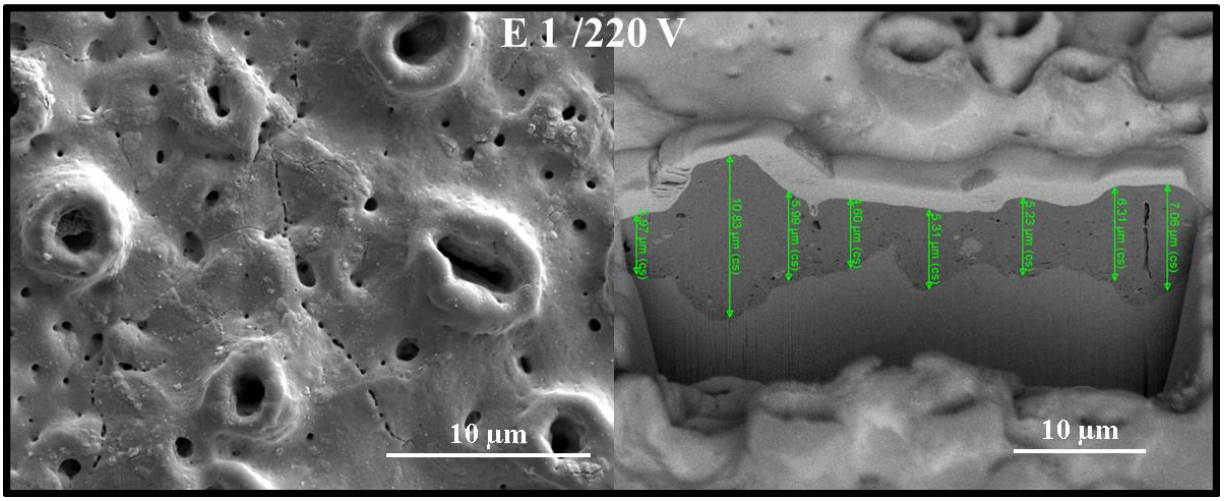

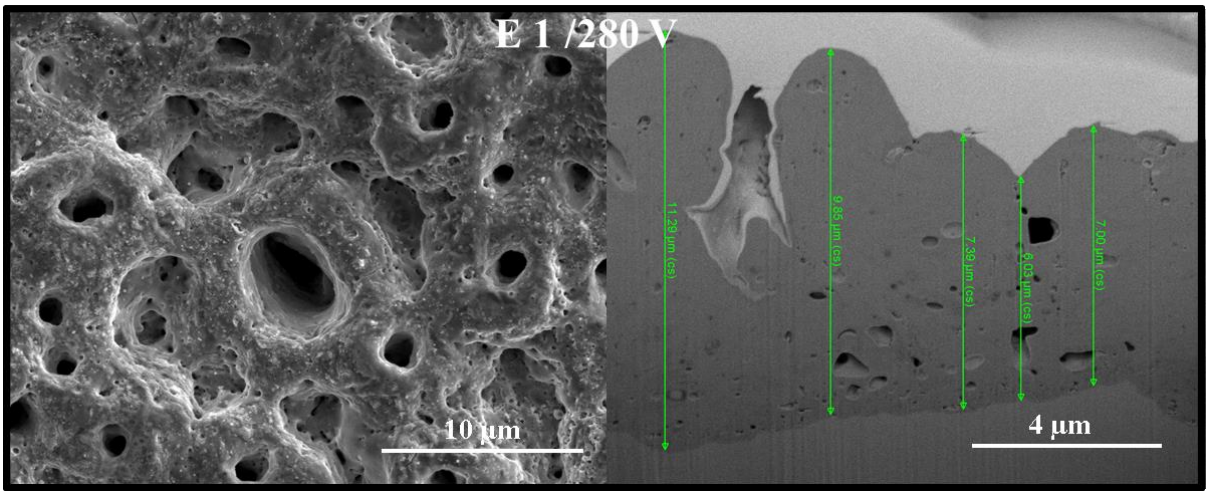

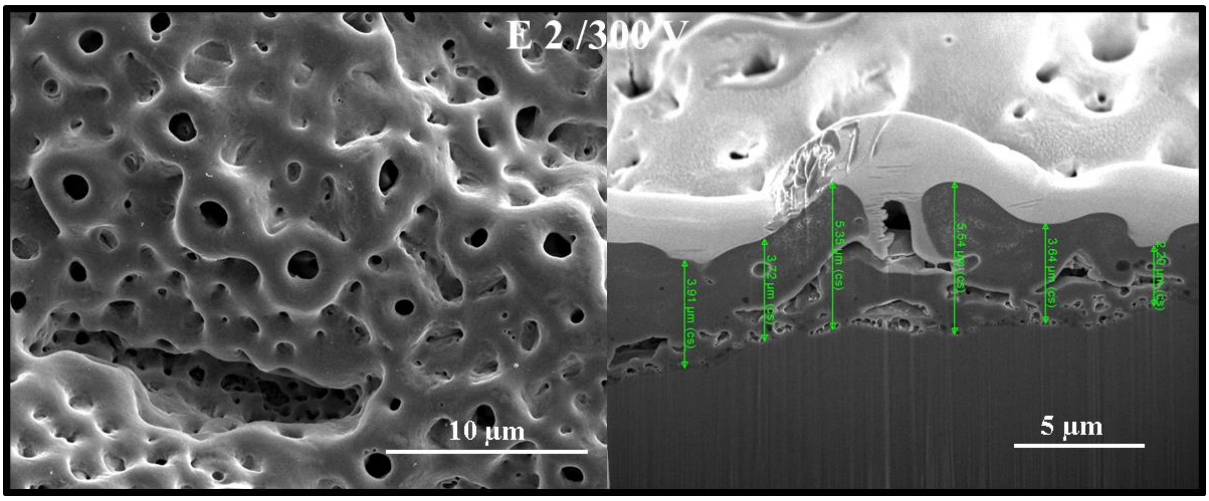
E 2 /300 V
10 µm
5 µm

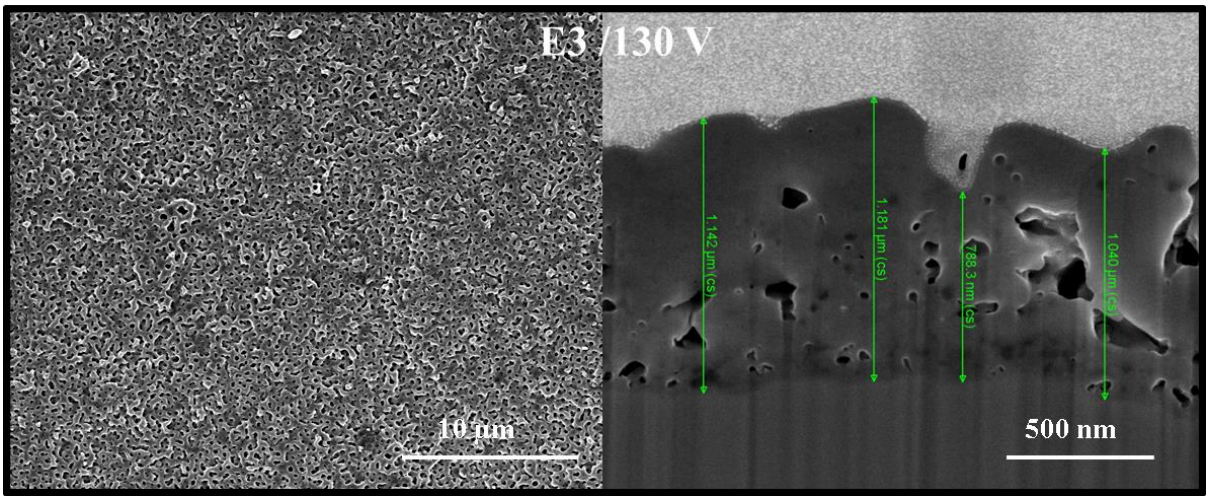
E3 /130 V
10 µm
500 nm

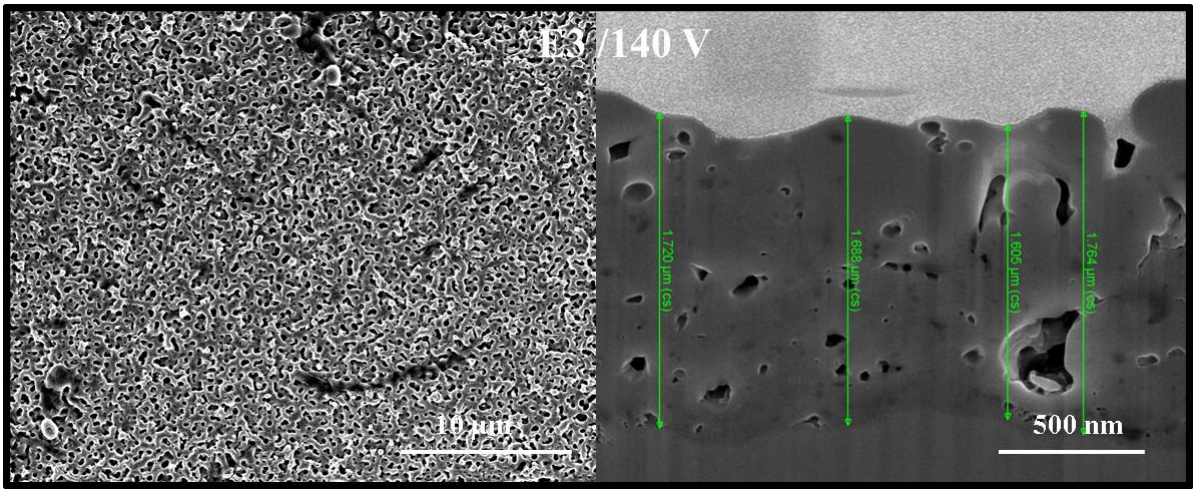
E3 /140 V
10 µm
500 nm

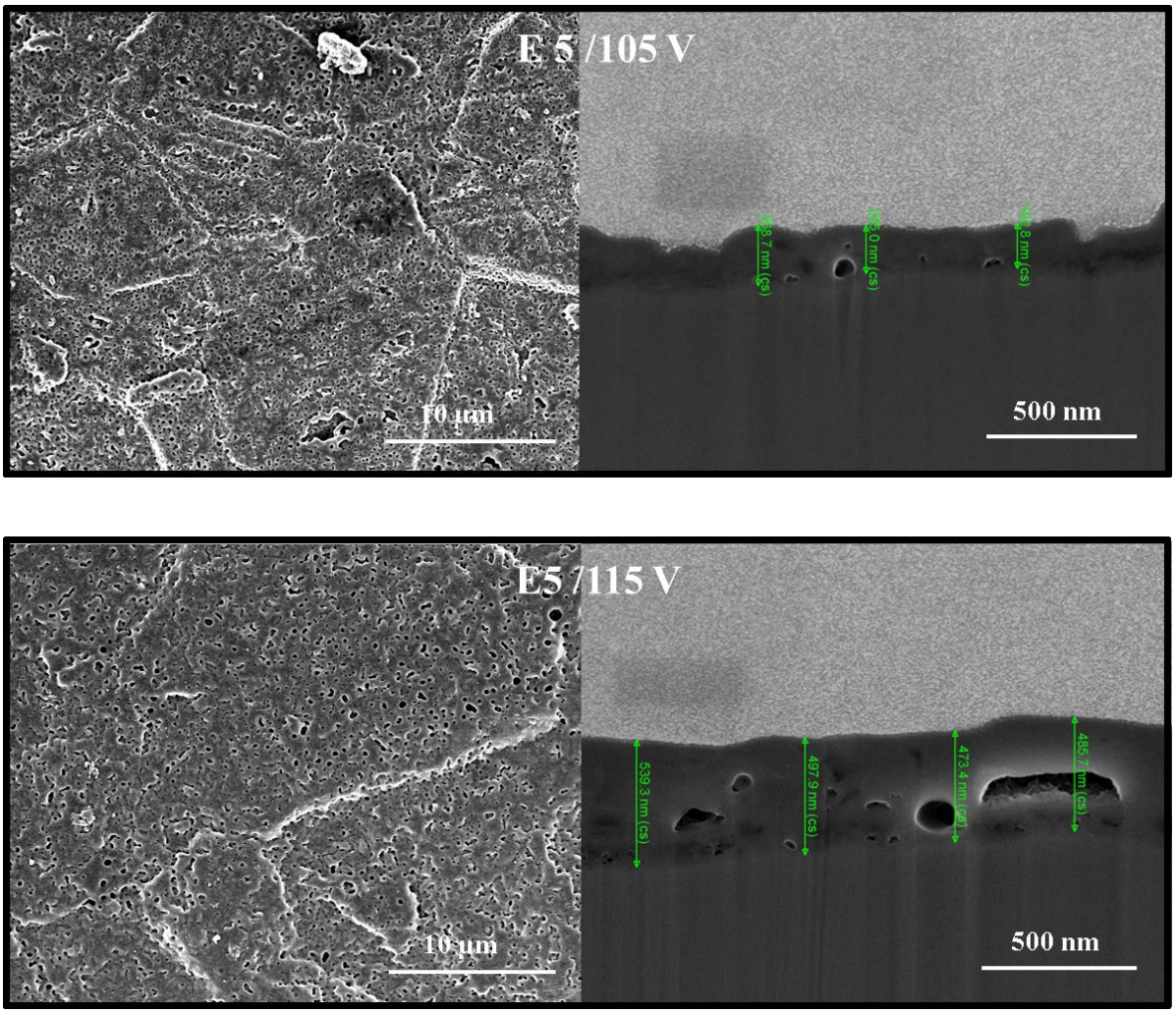

Fig. 1: SEM micrographs of the surface topographies of the PEO-treated titanium plates in the different electrolytes (E1 – E5): (left side) top view on the surface morphology with the characteristically pore-structures (magnification 10 µm) (right side) FIB cross-section of the as produced PEO-layers (different magnifications)

Tab. 2: Surface morphology and amounts in % of anatase and rutile of the PEO-treated surfaces (the remaining share up to 100% is titanium substrate) fabricated in different electrolytic systems

Electrolyte	Applied voltage /V	Pore size /µm	Layer thickness /µm	Phase amount anatase : rutile /%
E1	**220**	1.58 ± 0.31	6.29 ± 1.87	71(3)
	280	2.99 ± 0.51	14.37 ± 1.43	64(12) : 34(7)
E2	**300**	1.9 ± 0.7	3.86 ± 1.32	70(11)
E3	**130**	0.27 ± 0.09	1.04 ± 0.15	37(4) : 15(2)
	140	0.37 ± 0.11	1.69 ± 0.06	28(8) : 32(3)
E5	**105**	0.16 ± 0.02	0.22 ± 0.03	16.1(6)
	115	0.29 ± 0.09	0.5 ± 0.03	16.8(7) : 5(2)

Crystalline parts of anatase could be seen in the diffraction patterns for all PEO-samples, which were easily identified by the main reflection at 25.3 ° 2θ*(Cu)*. On the surface of the samples prepared in E1 and E3, recognizable crystalline parts of rutile were identified by the phase main reflection at

27.4° 2*θ(Cu)*. These crystalline parts of TiO_2 give an indication about the photocatalytic activity of the PEO-surfaces. Applying high voltages resulted in an increase in TiO_2-surface crystallinity. The alkaline electrolytes E2 and E5 produced a mainly anatase-covered surface without any clear rutile reflections, whereas the acidic electrolytes E1 and E3 resulted in surfaces that clearly show quantities of rutile. The strongest rutile reflection was seen for sample E1 at 280 V (Fig. 2). Increasing crystallinity with higher applied voltage caused by the resulting energy input of the intensified discharges over the surface is well known [31,42–45].

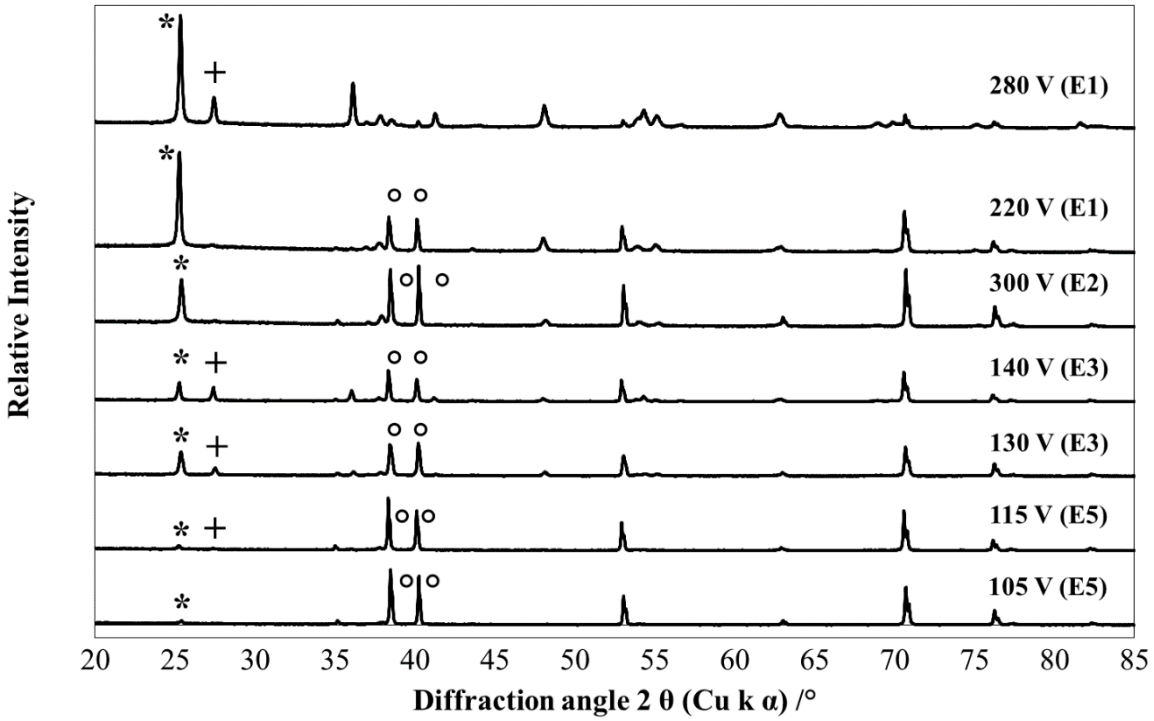

Fig. 2: XRD-pattern of PEO layers produced in the different electrolytes with the chosen applied voltage (important reflection peaks are marked; * anatase, + rutile, ° titanium)

3.2 Band gap measurement

Based on the XRD results of the PEO-surfaces, some measurements with UV-Vis diffuse reflectance spectroscopy were performed on the crystalline PEO-surfaces to determine the band gaps of the TiO_2 polymorphs. For the interpretation of the measured reflectance spectra, two systems, the so called TAUC-method [46] and DASF-method [47] were used. The reflectance spectra were first transformed into an absorbance spectrum using the Kubelka-Munk equation [48,49] and the band gaps were then calculated with the TAUC and DASF equations. Afterwards, both methods were applied to the absorbance spectra (Fig. 3) to determine the widths and the band gap type (indirect or direct) of the titania layers [50,51]. The absorbance spectra of the TAUC-plots for the samples prepared in the electrolytes E1, E2 and E3 in Fig. 3 show a clearly defined band gap. Thus, all samples show an expected band gap which are consistent with the calculations of the TAUC and DASF-method from Souri et al. [47]. For the samples prepared in E5, a refinement could not be carried out due to a slight

coloration of the surfaces. At this point, the PEO titania layers showed a direct band gap in contrast to the reported indirect band gap of anatase, which can clearly be seen in the comparison of the two methods in Fig .3. Anatase usually shows a band gap at almost E_g = 3.2 eV, while rutile shows a band gap at E_g = 3.0 eV [8], both TiO_2 polymorphs are semiconductors with an indirect band gap. The indirect band gap calculated with the TAUC-method does not fit to the data from the literature, while the direct band gaps given in Tab. 3 are closer to the data in the literature. The proportion of the rutile phase has a high influence on the band gap values, which shift to E_g = 3.0 eV. Madhusudan Reddy et al. [52] recognized a direct band gap of anatase nanoparticles with a small particle size of 5 - 10 nm, which results in an even smaller crystallite size. This could be one reason for the calculated direct band gap due to the relatively low crystallite sizes from 20 to 30 nm for all measured samples (Tab. 4). Due to the small crystallite size the specific surface area increases and the band gap shifts to a direct transition. Direct band gap semiconductors have a greater efficiency to absorb energy, because they contain an allowable transition from the conduction band to the valence band, whereas for indirect band gap semiconductors an additional phonon is necessary to shift the electron to the conduction band minimum, which reduces the efficiency drastically. As a result, these direct band gap materials can be used much more purposefully for specific applications [52].

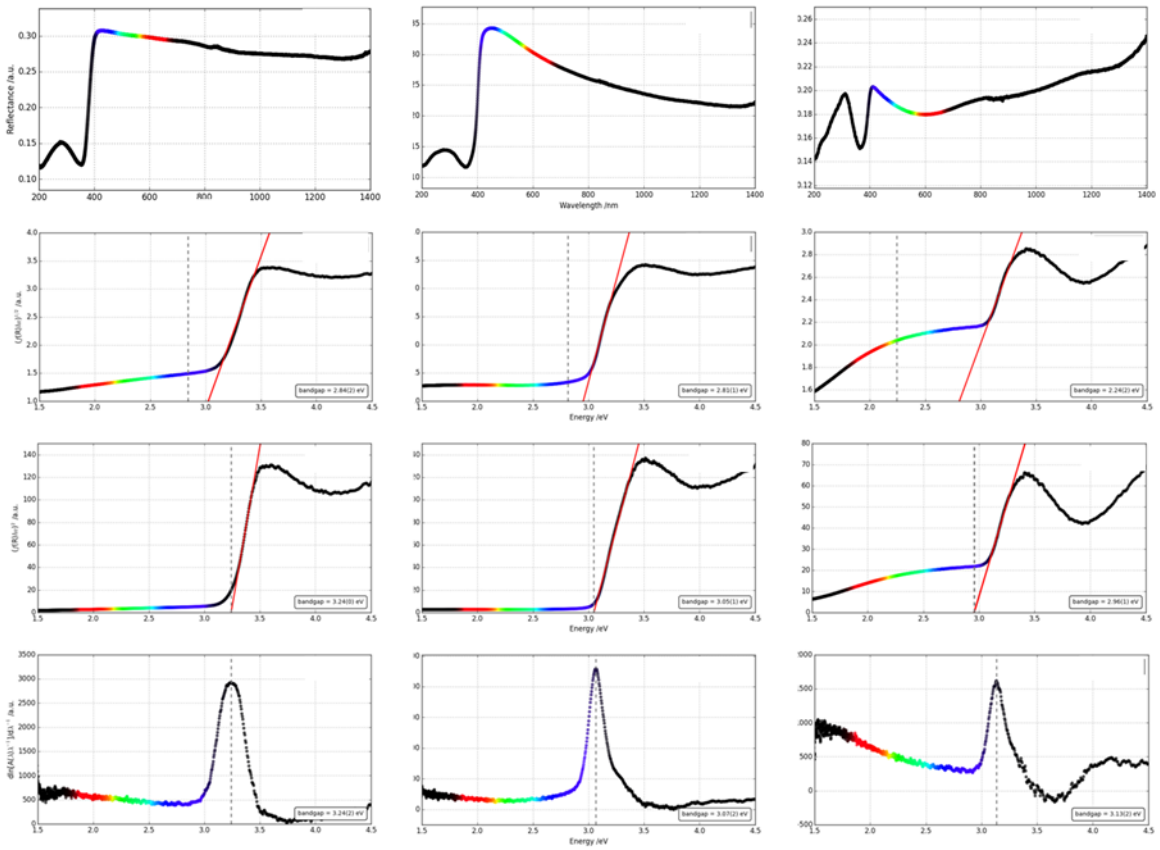

Fig. 3: UV/Vis absorbance spectra of the band gap measurement: Reflectance spectra (top), evaluated using the TAUC-method (middle rows; indirect and direct band gap) and DASF method (bottom). Plots of three PEO layers: first line sample E2 300 V, second line E1 280 V, third line E3 130 V. The solid lines show the fitted peaks and the dotted lines the bandgaps.

Tab. 3: Defined band gaps with the TAUC and DASF method for the PEO-treated surfaces for all electrolytes and applied voltages

Electrolyte	**E1**		**E2**	**E3**		**E5**	
Voltage /V	220	280	300	130	140	105	115
TAUC indirect /eV	2.76(1)	2.80(10)	2.90(1)	2.27(3)	2.71(1)	n.d.	n.d.
TAUC direct /eV	3.17(1)	3.05(10)	3.24(1)	2.96(3)	3.05(1)	n.d.	n.d.
DASF /eV	3.25(1)	3.10(1)	3.28(3)	3.16(1)	3.15(1)	n.d.	n.d.

n.d.: not definable

3.3 Photo degradation reactions

The degradation of two aqueous dye solutions was measured under UV irradiation by absorption spectroscopy. For these experiments the two widely used dyes methylene blue (MB) and rhodamine B (RB) were chosen. This carried out to compare the photocatalytic degradation in different solutions to exclude adsorption and desorption effects on the surfaces, which is a widely discussed effect. For these investigations crystalline PEO-surfaces with an optimal ratio of anatase to rutile compared to AEROXIDE® P25 (Evonik Degussa GmbH, Essen, Germany) (anatase 80%, rutile 20%) were used, analyzed with X-ray data Rietveld refinements. The respective crystalline phase compositions on the surfaces are given in Tab. 3. P25 is widely used to investigate photocatalytic activities as it is the most commonly used commercially available substance with a very high proven activity. Additionally, a PEO-sample was selected as dark reference, which was analyzed without UV-irradiation to determine the adsorption effects of the dye on the TiO_2 surface and is illustrated in each graph for each electrolyte. The decrease in absorption after storage in the dark is thus shown in the graphs and can visually subtract from the photocatalytic samples. The results from the photocatalytic experiments are shown in **Fehler! Verweisquelle konnte nicht gefunden werden.** and **Fehler! Verweisquelle konnte nicht gefunden werden.** for all PEO-treated samples at different voltages and in the four used electrolytes.

A high degradation rate of the used reference AEROXIDE® P25 can already be seen after 3 hours with a complete disappearance of absorption intensity. This is a typical reaction of P25 due to the interaction of its anatase and rutile quantities and the optimal average crystallite size of around 35 nm. For photocatalytic measurements, there is an ongoing discussion regarding adsorption and the splitting effects of dyes used at the soaked surfaces. Therefore, in addition to the dark reference, where the PEO-samples are not irradiated, an irradiated pure dye solution was examined as second reference. Slight absorbance degradation appeared for both pure dye solutions and the PEO-sample without UV irradiation. Nevertheless, both samples did not show a clear activity under UV irradiation or a strong decrease of absorption intensity. Thus, adsorption or desorption effects of the dyes at the surfaces and under UV-light can be refuted.

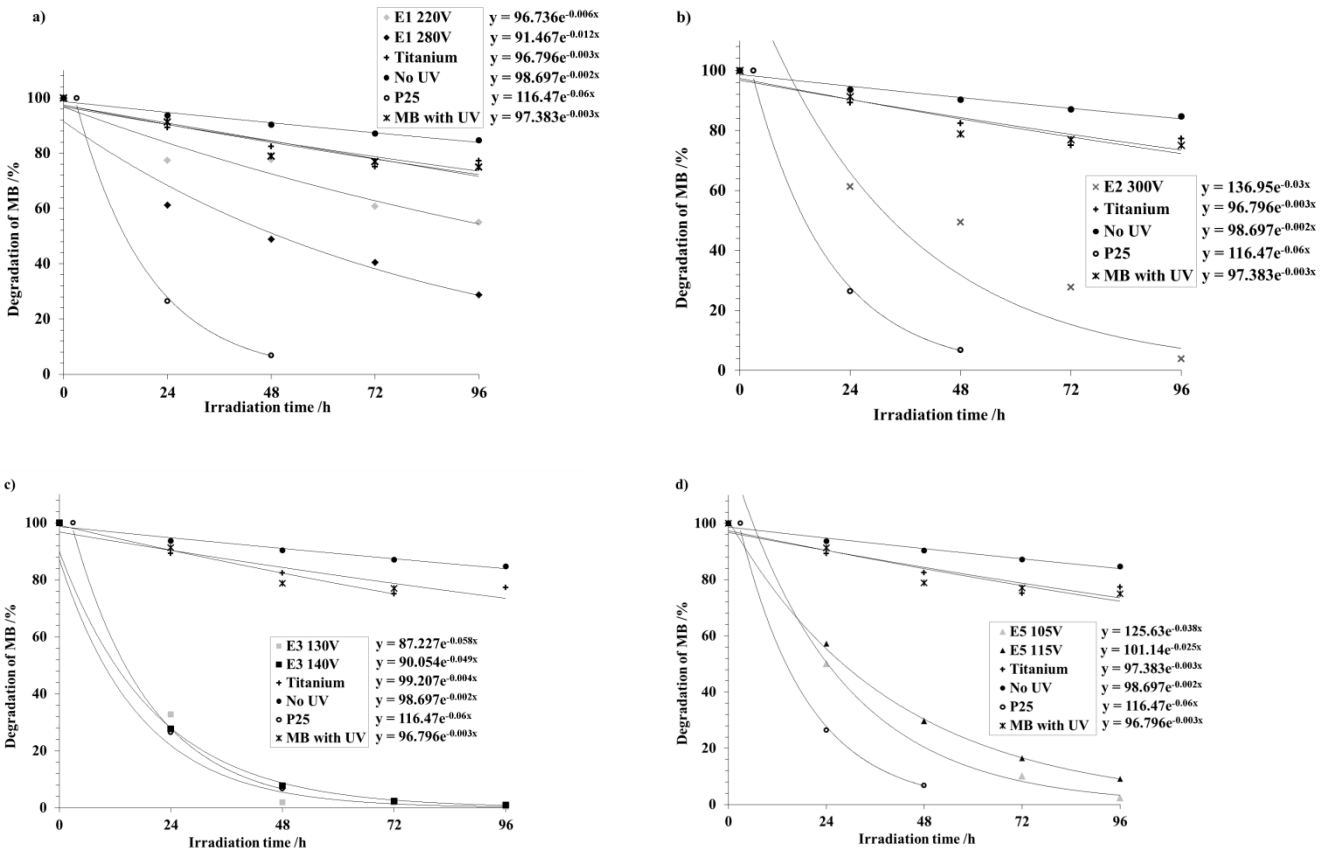

Fig. 4: Degradation rate of absorption intensity of MB: Values of the measured absorption maximum at 664 nm for the used electrolytes and the applied voltages a) E1 b) E2 c) E3 and d) E5

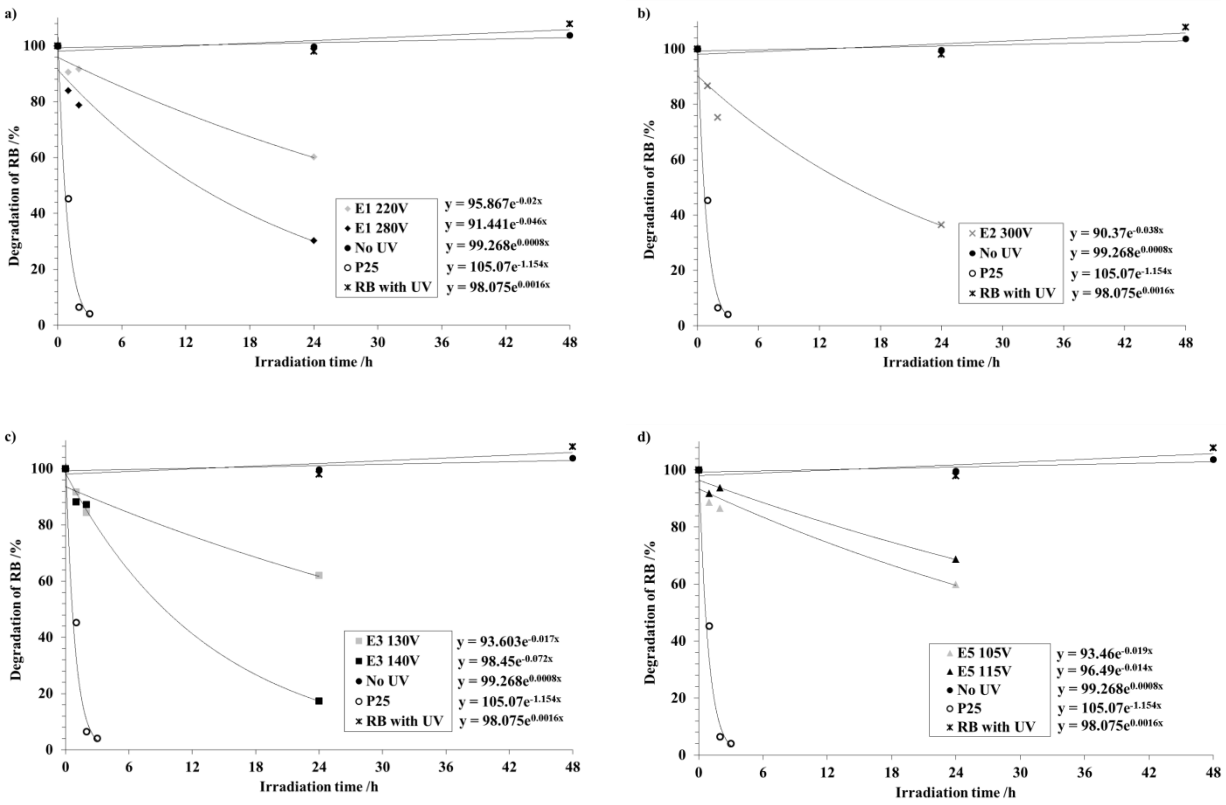

Fig. 5: Degradation rate of absorption intensity of RB: Values of the measured absorption maximum at 554 nm for the used electrolytes and the applied voltages a) E1 b) E2 c) E3 and d) E5

The samples prepared in the electrolytes E2, E3 and E5 showed the highest MB degradation rate after a 1-day illumination time (**Fehler! Verweisquelle konnte nicht gefunden werden.**). This behavior was also noticeable in RB for all these samples in nearly the same way (**Fehler! Verweisquelle konnte nicht gefunden werden.**). Both dyes showed a clear decrease in absorption intensity after 24 hours illumination time. The samples prepared in the electrolytes E1 in MB and E5 in RB showed a slightly lower activity compared to the other electrolytes. This behavior was clearer for the rhodamine B solution (**Fehler! Verweisquelle konnte nicht gefunden werden.**), whereby after 24 hours the degradation of the dye was only 25% of the starting intensity of the solution. For another exclusion of not desirable reactions the two dyes were compared in their photo degradation of the PEO-samples. Out of the two dyes, Rhodamine B showed significantly stronger photo degradation already after 24 hours and therefore is better suited for checking the photocatalytic activity of PEO-layers. In Fig 6 two degradation curves of the same sample in MB and RB is shown. The Rhodamine B dye shows a stronger degradation reaction after one and two hours (**Fehler! Verweisquelle konnte nicht gefunden werden.**). The samples soaked in methylene blue solution show only after 24 hours a decrease in absorption intensity. The illumination time for the experiments could thus be reduced while using RB as photocatalytic dye.

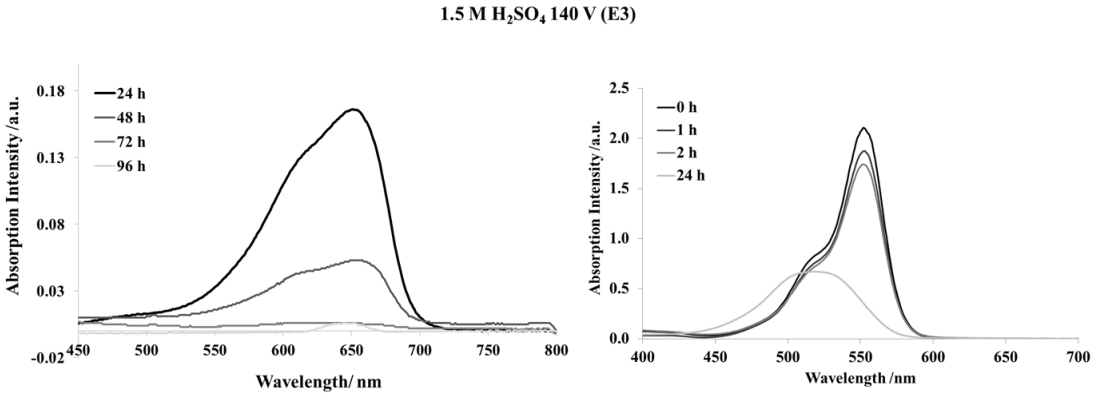

Fig. 6: Comparison of the two degradation spectra of sample E3 140 V (left side) MB after maximum illumination time of 96 hours (right side) RB after maximum illumination time of 24 hours

Mirelman et al. [33] reported a high photo-degradation rate with high quantities of anatase and a high coating thickness of the PEO-surfaces, which can be explained by the increased surface area available for the photocatalytic action of the produced UV photons. The increased photocatalytic activity can be seen for the samples with high applied voltages, which showed a high layer thickness (Tab. 2) and contained a high amount of anatase and some parts of rutile. Sample E3 140 V and sample E5 115 V exhibited both properties, such as high anatase content with a simultaneous increased layer thickness, which explains the strong photo activity of these samples. In the case of electrolyte E1 the layer thickness seems to be favorable for its photocatalytic activity and on the other hand for electrolyte E5 this seems to be unfavorable. The surfaces produces in electrolyte E5 show a relative low layer thickness compared to the other electrolytes but they show a comparable photo activity. That can be explained with the presence of the crystalline phases, which exist already at a very small layer thickness. Therefore in electrolyte E5 the crystallinity predominates over the surface area effects.

The photoactive surfaces treated in E3 contained a rutile amount of 15% (130 V), 31% (140 V) and a related ratio of 2:1 (130 V) and 1:1 (140 V) against the optimum ratio of both polymorphs of 3:1 in comparison to P25. The here demonstrated activity of all PEO-samples with high quantities of anatase and rutile could be an indication that not only the anatase phase causes photocatalytic activity and that PEO-surfaces are meant to contain some higher parts of rutile. During the PEO-process, in correlation with a high applied voltage causing a high oxide layer thickness, the photocatalytic activity and the associated crystallinity of the surfaces can be controlled using the nature of the electrolytes. This in turn leads to an increased surface area of the resulting low crystallite sizes of the TiO_2 phases, created by the high energy input of the plasma discharges. It has been reported [43,53] that an optimum crystallite size of 32 – 40 nm for TiO_2 surfaces enables photocatalytic activity. Accordingly, the crystallite sizes of anatase and rutile were investigated with Rietveld refinement (Diffrac Plus TOPAS, Bruker AXS GmbH, Karlsruhe, Germany) (Fig. 7). The PEO-surfaces showed a small

average crystallite size below 50 nm, which could be a reason for the photocatalytic activity of all surfaces. The anatase and rutile phases produced in E3 demonstrated an almost optimum crystallite size of around 40 nm. The samples produced at 130 V and 140 V in E3 showed an optimal crystallite size of almost 35 nm for both phases in contrast to the other investigated samples (Tab. 4), where average crystallite sizes were either below 30 nm or above 40 nm. Tiny crystallite sizes show less photocatalytic activity, because there are fewer possibilities for photo-excited interfaces [54,55]. Accordingly, the surface of "higher" crystallite sizes decreases, because of increased adsorption reactions of other molecules to the surface. Therefore, the photo-excited charges cannot reach the surface for photocatalytic activity [43,56]. Otherwise, the influence of layer thickness or pore sizes did not affect most the photocatalytic activity of the PEO-samples. Both samples with high or low layer thicknesses and pore sizes had the same results concerning the degradation rate (**Fehler! Verweisquelle konnte nicht gefunden werden.**, **Fehler! Verweisquelle konnte nicht gefunden werden.**). As previously reported, the occurrence of high amounts of crystalline phases on the surface and the presence of anatase and rutile phases in conjunction with a crystallite size between 30 and 40 nm has an effect on photocatalytic behavior. Especially for both samples of electrolyte E1 sample with a very high layer thickness and both samples of electrolyte E5 with a very small layer thickness. These samples show irrespective of their layer thicknesses a very good photocatalytic activity. All surfaces have a very high crystallinity observed in the XRD diffractogram and sample E1 280 V and E5 115 V contain also some amounts of crystalline rutile. In this case the crystallinity of the polymorphs seems to be more purposeful.

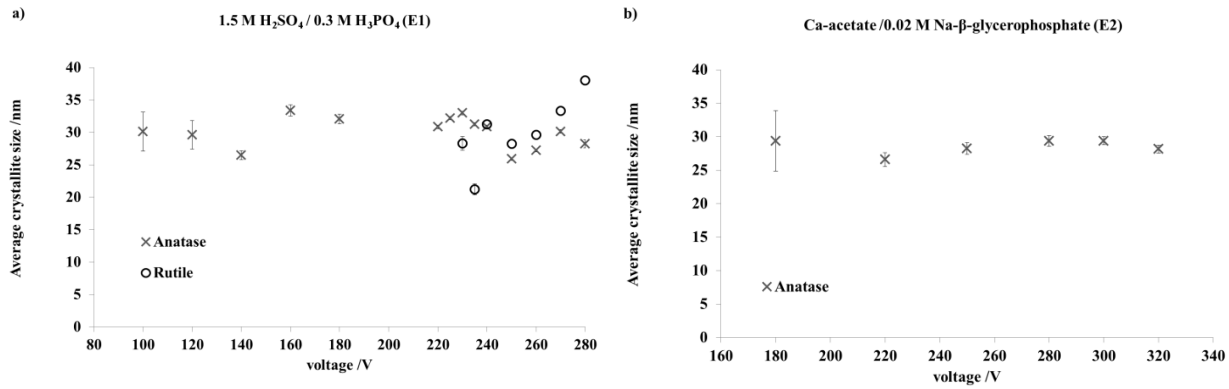

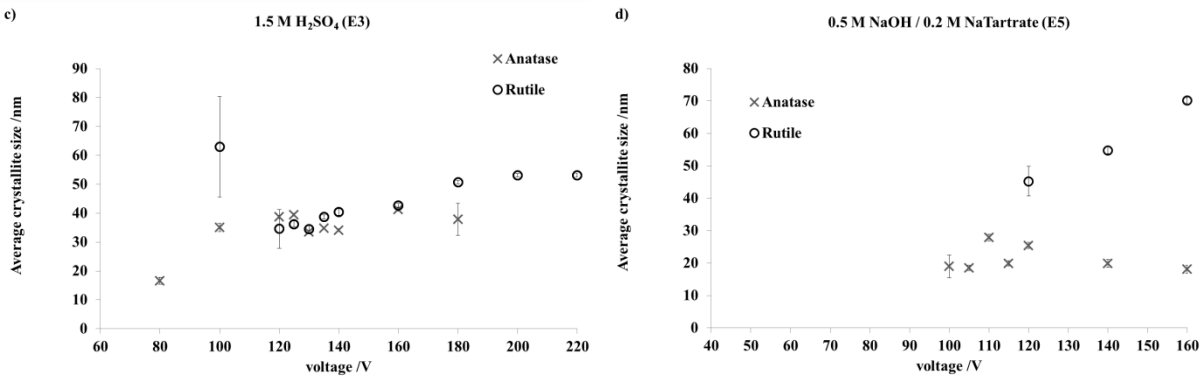

Fig. 7: Average crystallite sizes for anatase and rutile phases on the PEO surfaces produced in the electrolytes for each applied voltages a) E1 b) E2 c) E3 and d) E5

Tab. 4: Average crystallite sizes (L_{Vol}(IB)) of rutile and anatase on the PEO samples

Electrolyte		**E1**		**E2**	**E3**		**E5**	
Applied voltage /V		220	280	300	130	140	105	115
Average crystallite size /nm	Anatase	30.9(3)	28.3(6)	29.4(6)	33.5(6)	34.1(5)	27.9(10)	25.4(9)
	Rutile	-	38.1(10)	-	34.5(10)	40.4(10)	-	45.2(40)

4 Conclusion

The suitability of PEO-treated surfaces for photo-catalysis through the optimization of the TiO_2 surface crystallinity was investigated in this study. High amounts of the crystalline phases anatase and rutile were found throughout the oxide layers of PEO-treated titanium substrates. The different electrolytes affected these phases and enabled a control of the ratio between both phases from 100% anatase to 75% anatase and 25% rutile inside the PEO oxide layer. Using the PEO-process, it was possible to set purposeful surface conditions and layering properties for the photocatalytic suitability of the specimens. The investigations on the band gaps of the surfaces revealed a direct transition contrary to the reported indirect transition for TiO_2. The direct band gap could be clearly shown with the DASF method. This effect resulted from the very small crystallite sizes of TiO_2 polymorphs on the PEO-samples, namely 20 to 30 nm average crystallite size. It has been demonstrated that all PEO-surfaces show a photocatalytic degradation rate in contrast to an untreated titanium substrate with a natural amorphous oxide layer. This is consistent with the idea that high anatase and rutile contents and high levels of surface porosity with the characteristically PEO-structure optimize the surface area to form photons. It could also be argued that rutile particles in the layers can favor photocatalytic activity, as seen for the samples E1 280 V and E5 115 V, but a high proportion of anatase with a crystallite size of 30 nm appears to be the most effective at strengthening the photocatalytic properties. The small crystallite size maximizes the surface area on which the catalytic reaction can occur. Both effects of optimization using the PEO-process are a possible way to support photocatalytic activity.

Acknowledgement

The authors want to thank Michael Teck (Solid State Chemical Crystallography, University of Bremen) for his assistance and helpful inputs to the photocatalytic measurements. This research did not receive any specific grant from funding agencies in the public, commercial, or not-for-profit sectors.

5 References

[1] M.A. Fox, Photocatalytic Oxidation of Organic Substrates, in: Proc. NATO ASI Int. Conf. Photocatal. Environ. Trends Appl., In: Schiavello M (ed.), Palermo, Kluwer, Dodrecht, 1988: pp. 445–467.

[2] J.M. Macak, M. Zlamal, J. Krysa, Self-Organized TiO2 Nanotube Layers as Highly Efficient Photocatalysts, 6 (2007) 300–304. doi:10.1002/smll.200600426.

[3] E.M. Saggioro, A.S. Oliveira, T. Pavesi, C.G. Maia, L. Filipe, V. Ferreira, J.C. Moreira, Use of Titanium Dioxide Photocatalysis on the Remediation of Model Textile Wastewaters Containing Azo Dyes, (2011) 10370–10386. doi:10.3390/molecules161210370.

[4] M. Gratzel, Energy Resources through Photochemistry and Catalysis, Academic Press, New York, 1983.

[5] N. Serpone, Ezio Pelizzetti, Photocatalysis, Wiley, New York, 1989.

[6] O.K. Varghese, M. Paulose, K. Shankar, G.K. Mor, C.A. Grimes, Water-photolysis properties of micron-length highly-ordered titania nanotube-arrays, J. Nanosci. Nanotechnol. 5 (2005) 1158.

[7] N.K. Allam, C.A. Grimes, Photoelectrochemical and water photoelectrolysis properties of ordered TiO2 nanotubes fabricated by Ti anodization in fluoride-free HCl electrolytes, (2008). doi:10.1039/b718580d.

[8] A. Fujishima, K. Hashimoto, T. Watanabe, TiO2 photocatalysis: fundamentals and applications, Tokyo Bkc, Tokyo, 1999.

[9] D.G. Fu, Y. Zhang, X. Wang, J.Z. Liu, Z.H. Lu, Surface Second Order Optical Nonlinearity of Titanium Dioxide Sized in Nanometer Range, Chem. Lett. (2001) 328–329.

[10] F.A. Grant, Properties of Rutile (Titanium Dioxide), Rev. Mod. Phys. 31 (1959) 646.

[11] H.P.R. Frederiske, Recent Studies on Rutile (TiO2), J. Appl. Phys. 32 (1961) 2211.

[12] A.H. Abdullah, U.I. Gaya, Heterogeneous photocatalytic degradation of organic contaminants over titanium dioxide: A review of fundamentals, progress and problems, J. Photochem. Photobiol., C Photochem. Rev. 9 (2008) 1–12.

[13] C.B. Mendive, T. Bredow, A. Feldhoff, M. Blesa, D. Bahnemann, Adsorption of oxalate on anatase (100) and rutile (110) surfaces in aqueous systems: experimental results vs. theoretical predictions, Phys. Chem. Chem. Phys. 11 (2009) 1794–1808. doi:10.1039/b814608j.

[14] M. Kaneko, I. Okura, Photocatalysis: Science and Technology (Biological and Medical Physics Series), Springer, Berlin, 2007.

[15] M.R. Hoffmann, S.T. Martin, W. Choi, D.W. Bahnemannt, Environmental Applications of Semiconductor Photocatalysis, Chem. Rev. 95 (1995) 69–96.

[16] A.Y. Ahmed, T. Kandiel, T. Oekermann, D. Bahnemann, Photocatalytic Activities of Different Well-defined Single Crystal, J. Phys. Chem. Lett. 2 (2011) 2461–2465. doi:10.1021/jz201156b.

[17] W. Kim, T. Tachikawa, G.H. Moon, T. Majima, W. Choi, Molecular-level understanding of the photocatalytic activity difference between anatase and rutile nanoparticles, Angew. Chemie - Int. Ed. 53 (2014) 14036–14041. doi:10.1002/anie.201406625.

[18] M.L. Kääriäinen, T.O. Kääriäinen, D.C. Cameron, Titanium dioxide thin films, their structure

and its effect on their photoactivity and photocatalytic properties, Thin Solid Films. 517 (2009) 6666–6670. doi:10.1016/j.tsf.2009.05.001.

[19] S.K. Poznyak, D. V. Talapin, A.I. Kulak, Electrochemical oxidation of titanium by pulsed discharge in electrolyte, J. Electroanal. Chem. 579 (2005) 299–310. doi:10.1016/j.jelechem.2005.03.002.

[20] V. Ramaswamy, N.B. Jagtap, S. Vijayanand, D.S. Bhange, P.S. Awati, Photocatalytic Decomposition of Methylene Blue on Nano-Crystalline Titania Prepared by Different Methods, Mater. Res. Bull. 5 (2008) 1145–1152.

[21] J. Bennani, R. Dillert, T.M. Gesing, D. Bahnemann, Physical properties, stability, and photocatalytic activity of transparent TiO2/SiO2 films, Sep. Purif. Technol. 67 (2009) 173–179. doi:10.1016/j.seppur.2009.03.019.

[22] P. Evans, T. English, D. Hammond, M.E. Pemble, D.W. Sheel, The Role of SiO2 Barrier Layers in Determin-ing the Structure and Photo-Catalytic Activity of TiO2 Films Deposited on Stainless Steel, Appl. Catal. 2 (2007) 140–146.

[23] J. Mungkalasiri, L. Bedel, F. Emieux, J. Doré, F.N.R. Renaud, F. Maury, DLI-CVD of TiO2-Cu Antibacterial Thin Films: Growth and Characterization, Surf. Coatings Technol. 6–7 (2009) 887–892.

[24] W. Mc Niell, G. Nordbloom, Method of making cadmium niobate, US2854390 A, 1958.

[25] W. Mc Niell, G. Nordbloom, Anodic spark reaction processes and articles, US 3293158 A, 1966.

[26] G. Markov, G. Markova, The formation method of anodic electrolytic condensation, 526961, 1976.

[27] A.V. Nikolaev, G.A. Markov, B.I. Peshchevitskij, In Russian, Izv. SO ANSSSR. Ser. Khim. Nauk 5. 5 (1977) 32.

[28] X. Liu, P.K. Chu, C. Ding, Surface nano-functionalization of biomaterials, Mater. Sci. Eng. R Reports. 70 (2010) 275–302. doi:10.1016/j.mser.2010.06.013.

[29] T. Akatsu, Y. Yamada, Y. Hoshikawa, T. Onoki, Y. Shinoda, F. Wakai, Multifunctional porous titanium oxide coating with apatite forming ability and photocatalytic activity on a titanium substrate formed by plasma electrolytic oxidation, Mater. Sci. Eng. C. 33 (2013) 4871–4875. doi:10.1016/j.msec.2013.08.003.

[30] Y. Mizukoshi, N. Masahashi, Fabrication of a TiO2 photocatalyst by anodic oxidation of Ti in an acetic acid electrolyte, Surf. Coatings Technol. 240 (2014) 226–232. doi:10.1016/j.surfcoat.2013.12.030.

[31] M.R. Bayati, F. Golestani-Fard, A.Z. Moshfegh, The effect of growth parameters on photo-catalytic performance of the MAO-synthesized TiO2 nano-porous layers, Mater. Chem. Phys. 120 (2010) 582–589. doi:10.1016/j.matchemphys.2009.12.005.

[32] M.R. Bayati, F. Golestani-Fard, A.Z. Moshfegh, How photocatalytic activity of the MAO-grown TiO2 nano/micro-porous films is influenced by growth parameters?, Appl. Surf. Sci. 256 (2010) 4253–4259. doi:10.1016/j.apsusc.2010.02.011.

[33] L.K. Mirelman, J.A. Curran, T.W. Clyne, The production of anatase-rich photoactive coatings by plasma electrolytic oxidation, Surf. Coatings Technol. 207 (2012) 66–71. doi:10.1016/j.surfcoat.2012.05.076.

[34] A. Houas, H. Lachheb, M. Ksibi, E. Elaloui, C. Guillard, J.-M. Herrmann, Photocatalytic

degradation pathway of methylene blue in water, Appl. Catal. B Environ. 31 (2001) 145–157. doi:10.1016/S0926-3373(00)00276-9.

[35] A.E.R. Friedemann, T.M. Gesing, P. Plagemann, Electrochemical rutile and anatase formation on PEO surfaces, Surf. Coat. Technol. 315 (2017) 139–149. doi:10.1016/j.surfcoat.2017.01.042.

[36] P. Wilhelm, D. Stephan, Photodegradation of rhodamine B in aqueous solution via SiO2@TiO2 nano-spheres, J. Photochem. Photobiol. A Chem. 185 (2007) 19–25. doi:10.1016/j.jphotochem.2006.05.003.

[37] H.J. Oh, J.H. Lee, Y. Jeong, Y.J. Kim, C.S. Chi, Microstructural characterization of biomedical titanium oxide film fabricated by electrochemical method, Surf. Coatings Technol. 198 (2005) 247–252. doi:10.1016/j.surfcoat.2004.10.029.

[38] S. Ito, K. Koizuka, M. Hirochi, T. Onaka, H.M.T. Haneda, Anodic Oxidation of Titanium in Phosphoric Acid-Sulfuric Acid System Electrolytic Bath, J. Japan Soc. Colour Mater. 61 (1988) 599–605.

[39] Y.K. Shin, W.S. Chae, Y.W. Song, Y.M. Sung, Formation of titania photocatalyst films by microarc oxidation of Ti and Ti-6Al-4V alloys, Electrochem. Commun. 8 (2006) 465–470. doi:10.1016/j.elecom.2006.01.003.

[40] N. Kim, K. H.; Ramaswamy, Electrochemical surface modification of titanium in dentistry., Dent. Mat. J. 28 (2009) 20–36.

[41] D. Quintero, O. Galvis, J.A. Calderón, J.G. Castaño, F. Echeverría, Effect of electrochemical parameters on the formation of anodic films on commercially pure titanium by plasma electrolytic oxidation, Surf. Coatings Technol. 258 (2014) 1223–1231. doi:10.1016/j.surfcoat.2014.06.058.

[42] Z. Su, L. Zhang, F. Jiang, M. Hong, Formation of crystalline TiO2 by anodic oxidation of titanium, Prog. Nat. Sci. Mater. Int. 23 (2013) 294–301. doi:10.1016/j.pnsc.2013.04.004.

[43] Y. Mizukoshi, N. Masahashi, Photocatalytic Activities and Crystal Structures of Titanium Dioxide by Anodization: Their Dependence upon Current Density, Mater. Trans. 51 (2010) 1443–1448. doi:10.2320/matertrans.M2010106.

[44] M. V. Diamanti, M.P. Pedeferri, Effect of anodic oxidation parameters on the titanium oxides formation, Corros. Sci. 49 (2007) 939–948. doi:10.1016/j.corsci.2006.04.002.

[45] C.S. Dunleavy, J.A. Curran, T.W. Clyne, Self-similar scaling of discharge events through PEO coatings on aluminium, Surf. Coatings Technol. 206 (2011) 1051–1061. doi:10.1016/j.surfcoat.2011.07.065.

[46] J. Tauc, R. Grigorovici, V. A, Optical properties and electronic structure of amorphous germanium, Phys. Status Solidi. 15 (1996) 627–637. doi:10.1002/pssb.19660150224.

[47] D. Souri, Z.E. Tahan, A new method for the determination of optical band gap and the nature of optical transitions in semiconductors, Appl. Phys. B Lasers Opt. 119 (2015) 273–279. doi:10.1007/s00340-015-6053-9.

[48] P. Kubelka, F. Munk, Ein Beitrag zur Optik der Farbanstriche, Zeitschrift Für Tech. Phys. 12 (1931) 593–601.

[49] V. Džimbeg-malčić, Ž. Barbarić-mikočević, K. Itrić, Kubelka-Munk Theory in Describing Optical Properties of Paper (1), Tech. Gaz. 18 (2011) 117–124. doi:10.1017/CBO9781107415324.004.

[50] A. Kirsch, M.M. Murshed, M. Schowalter, A. Rosenauer, T.M. Gesing, Nanoparticle precursor into polycrystalline Bi2Fe4O9: An evolutionary investigation of structural, morphological, optical and vibrational properties., J. Phys. Chem. C. 120 (2016) 18831–18840.

[51] M. Teck, M.M. Murshed, M. Schowalter, N. Lefeld, H.K. Grossmann, T. Grieb, T. Hartmann, L. Robben, A. Rosenauer, L. Mädler, T.M. Gesing, Structural and spectroscopic comparison between polycrystalline, nanocrystalline and quantum dot visible light photo-catalyst Bi2WO6., J. Solid State Chem. (2017). submitted.

[52] K.M. Reddy, S. V. Manorama, A.R. Reddy, Bandgap studies on anatase titanium dioxide nanoparticles, Mater. Chem. Phys. 78 (2003) 239–245. doi:10.1016/S0254-0584(02)00343-7.

[53] M. Inagaki, R. Nonaka, B. Tryba, A.W. Morawski, Dependence of photocatalytic activity of anatase powders on their crystallinity, Chemosphere. 64 (2006) 437–445. doi:10.1016/j.chemosphere.2005.11.052.

[54] H. Kominami, J. Kato, M. Kohno, Y. Kera, B. Ohtani, Photocatalytic Mineralization of Acetic Acid in Aerated Aqueous Suspension of Ultra-highly Active Titanium(IV) Oxide Prepared by Hydrothermal Crystallization in Toluene, Chem. Lett. 12 (1996) 1051–1052.

[55] F. Amano, O.-O. Preto-Mahaney, Y. Terada, T. Yasumoto, T. Shibayama, B. Ohtani, Decahedral Single-Crystalline Particles of Anatase Titanium(IV) Oxide with High Photocatalytic Activity, Chem. Mat. 21 (2009) 2601–2603. doi:DOI: 10.1021/cm9004344.

[56] O. Carp, C.L. Huisman, A. Reller, Photoinduced reactivity of titanium dioxide, Prog. Solid State Chem. 32 (2004) 33–177.